ELSEVIER Applied Mathematics and Computation 134 (2003) 271–291
APPLIED MATHEMATICS AND COMPUTATION
www.elsevier.com/locate/amc

A numerical scheme for the simulation of blow-up in the nonlinear Schrödinger equation

Salvador Jiménez [a], Ignacio M. Llorente [b], Ana M. Mancho [c], Víctor M. Pérez-García [d,*], Luis Vázquez [e]

[a] *Departamento de Matemática y Física Aplicada, Universidad Alfonso X el Sabio, 28691 Madrid, Spain*
[b] *Departamento de Arquitectura de Computadores y Automática, Facultad de CC. Físicas, Universidad Complutense, 28040 Madrid, Spain*
[c] *Centro de Astrobiología (Associate Member of NASA Astrobiology Institute), CSIC-INTA, Ctra. Ajalvir, km. 4, 28850 Torrejón de Ardoz, Madrid, Spain*
[d] *Departamento de Matemáticas, Escuela Técnica Superior de Ingenieros Industriales, Universidad de Castilla-La Mancha, Avenida de Camilo Jose Cela 3, 13071 Ciudad Real, Spain*
[e] *Departamento de Matemática Aplicada, Facultad de Informática, Universidad Complutense, 28040 Madrid, Spain*

Abstract

We present a self-adaptive multigrid version of a conservative finite difference scheme useful for the study of collapse processes in nonlinear Schrödinger equations (NLSEs). As an example we study the character of the focusing singularity of the two-dimensional critical NLSE.

Keywords: Finite difference schemes; Blow-up; Nonlinear Schrödinger equations; Multigrid methods

* Corresponding author.
E-mail address: vperez@ind-cr.uclm.es (V.M. Pérez-García).

0096-3003/02/$ - see front matter
PII: S0096-3003(01)00282-X

1. Introduction

The nonlinear schrödinger equation (NLSE) in its many version is one of the most important models of mathematical physics, with applications in different fields such as plasma physics, nonlinear optics, water waves bimolecular dynamics, to cite only a few cases (see e.g. [1–4]). In many of those examples the equation appears as an asymptotic limit for a slowly varying dispersive wave envelope propagating in a nonlinear medium. These are not the only examples of applications of the NLSE, in fact a new burst of interest on this equation has been motivated by the recent achievement of Bose–Einstein condensation using ultracold neutral bosonic gases. In this case the NLSE is obtained as a mean field model for the dynamics near $T = 0$ [5]. In this framework, the realization of experimental systems with unstable (collapsing) properties [6] has further stimulated theoretical research on collapse phenomena [7] in the framework of models based on NLSEs.

It is our objective in this paper to present a self-adaptive multigrid version of a conservative finite difference scheme useful for the study of collapse processes in NLSEs, whose general form is

$$\mathrm{i}\Psi_t + \Delta\Psi + f(|\Psi|^2)\Psi = 0, \tag{1}$$

$$\Psi(\mathbf{x}, 0) = \Psi_0(\mathbf{x}), \tag{2}$$

where $\Delta = \partial^2/\partial x_1^2 + \cdots + \partial^2/\partial x_n^2$. Many forms of the function f appear in the applications. The most classical is $f(|\Psi|^2) = |\Psi|^2$ which leads to the usual collapse phenomenon. In nonlinear optics many versions of the so-called saturable nonlinearities appear, e.g. $f(|\Psi|^2) = |\Psi|^2 - \alpha|\Psi|^4$, $f(|\Psi|^2) = |\Psi|^2/(1 + |\Psi|^2)$. In the field of applications to Bose–Einstein condensation other type of nonlinear terms are possible such as $f(|\Psi|^2) = \int K(\mathbf{r} - \mathbf{x}')|\Psi(\mathbf{x}')|^2 \mathrm{d}\mathbf{x}'$, $f(|\Psi|^2) = |\Psi|^2 - i\alpha|\Psi|^4$. These are only some examples of the many forms the nonlinear term may have, each one giving rise to different phenomena such as collapse inhibition, etc. However, when collapse phenomena are involved one must be very careful with the related numerical analysis of the problem.

When the nonlinear function f is real the system has several conserved quantities which include the energy (Hamiltonian), whose explicit form is,

$$H \equiv E(\Psi) = \int \mathrm{d}^n\mathbf{x}|\vec{\nabla}\Psi|^2 - \int \mathrm{d}^n\mathbf{x}G(\Psi) = K(\Psi) + U(\Psi). \tag{3}$$

Under very general conditions of f it can be shown that the Cauchy problem has a unique local solution $\Psi(t, \mathbf{x})$, with $t \in [0, T)$ in the energy space X which is usually the Sobolev space $H^1(R^n)$ [8]. A basic problem is whether this solution can be continued to $T = \infty$, that is, to global solution in X. When the solution is not global we speak of collapse or blow-up. When the solutions are

global but develop "strong peaks" (measured in some norm) during evolution, one speaks of quasi-collapse processes. In the quasi-collapsing examples there is not a full collapse (mathematically the solution is global in time), but the amplitude grows in a localized spatial region leading to a spike of the amplitude of the solution, which is difficult to describe using standard numerical schemes. This is also the case during real collapse processes, where the scheme must be able to integrate the solution up to the vicinity of the collapse point and even to detect the existence of the singularity, a fact which is not known a priori in some cases.

These facts have motivated us to design a fast numerical scheme easy to implement with many desirable properties which is specially suitable for the analysis of collapse processes. The purpose of this paper is to study this numerical scheme and its multigrid implementation for the simplest case of the cubic nonlinearity.

Our plan is as follows: First, the numerical scheme is presented in Section 2, secondly, we study its advanced implementation using multigrid techniques in Section 3. As an example of application we have studied a well-documented case in Section 4, which is the blow-up of the two-dimensional cubic NLSE. For this problem there is a vast literature concerning the conditions under which collapse exists and the way the solutions collapse [4]. Finally, in Section 5 we summarize our conclusions.

2. The numerical scheme: Conservation properties, stability and convergence

2.1. Finite difference scheme and conserved quantities

For the sake of simplicity we will concentrate in this work on radially symmetric problems in two dimensions so that the Cauchy problem we are interested on is

$$\mathrm{i}\frac{\partial \Psi}{\partial t}+\frac{1}{r}\frac{\partial}{\partial r}\left(r\frac{\partial}{\partial r}\right)\Psi+f(|\Psi|^2)\Psi=0, \tag{4}$$

with initial data $\Psi_0(r)$ on R^+ and boundary conditions

$$\left.\frac{\mathrm{d}\Psi}{\mathrm{d}r}\right|_{r=0}=0, \quad \lim_{r\to\infty}\Psi(t,r)=0. \tag{5}$$

This model has been shown to retain most of the interesting features of the critical collapse phenomenon even in systems without symmetry [9]. This equation has two conserved quantities, namely the energy and L^2 norm, which are,

$$E = 2\pi \int \mathrm{d}r\, r \left[-\left| \frac{\partial \Psi}{\partial r} \right|^2 + G(|\Psi|^2) \right], \tag{6a}$$

$$N = 2\pi \int \mathrm{d}r\, r |\Psi(r,t)|^2. \tag{6b}$$

Many numerical schemes are used to simulate the NLSE [10,11] including finite difference [12–18], finite element [19,20] and pseudoespectral [21–25] schemes. It is commonly accepted that to simulate Hamiltonian wave processes symplectic and conservative schemes are preferred over conventional ones because of their better global stability and long time behavior. In our case we have chosen to follow the ideas of [15], because the construction of a three-level difference conservative scheme allows the discrete problem to be linearly implicit and thus a computationally economic choice while preserving some integral quantities.

To approximate the above problem using finite differences we define the grid $\Omega_h = \{jh\}_{j=0}^{Mh}$ and the time step τ. The numerical scheme we propose for the integration of Eq. (4) is the following,

$$\begin{aligned} &\mathrm{i}\left(\frac{\psi_j^{n+1} - \psi_j^{n-1}}{2\tau} \right) + \frac{\psi_{j+1}^{n+1} - 2\psi_j^{n+1} + \psi_{j-1}^{n+1}}{2h^2} + \frac{\psi_{j+1}^{n-1} - 2\psi_j^{n-1} + \psi_{j-1}^{n-1}}{2h^2} \\ &\quad + \frac{1}{hj}\left(\frac{\psi_{j+1}^{n+1} - \psi_{j-1}^{n+1}}{4h} \right) + \frac{1}{hj}\left(\frac{\psi_{j+1}^{n-1} - \psi_{j-1}^{n-1}}{4h} \right) + \frac{1}{2} f(|\psi_j^n|^2)(\psi_j^{n+1} + \psi_j^{n-1}) \\ &\quad = 0, \end{aligned} \tag{7}$$

where ψ_j^n is an approximation to the solution at the point $r_j = jh$, $t_n = n\tau$. Scheme (7) is a finite difference three-level linearly implicit scheme. To compute the solution at the second level in time it is necessary to use any other method. In our case we have used a second-order nonlinearly implicit Crank–Nicholson method, which is solved by iteration. In fact, to minimize the effect of the nonconservative character of the Crank–Nicholson scheme we have initialized the scheme with a time step ten times smaller than the original one and then scheme (7) is applied to iterate the remaining 9 steps to complete the second time step. Performing Taylor expansions around ψ_j^n, which is the central value, it can be seen that due to the symmetry of the expression the truncation error of the scheme is $\mathrm{O}(\tau^2 + h^2)$ (see for instance [26] for a similar result).

The most striking property of the scheme is that it has a discrete analogous of Eq. (6b) that is conserved exactly, whenever the continuous one is also conserved. The discrete conservation law is obtained following the ideas described in [27]. Multiplying (7) by $(\bar{\psi}_j^{n+1} + \bar{\psi}_j^{n-1})/2$, where the bar denotes complex conjugation. Taking the imaginary part and summing for all values of

j in the spatial mesh, and rearranging properly the terms, one gets that N^n is conserved by the time iteration, being:

$$N^n = \sum_{j=1}^{M} h(hj)\frac{|\psi_j^{n+1}|^2 + |\psi_j^n|^2}{2}. \tag{8}$$

Special conditions are necessary to be fulfilled for all n considered:

$$\psi_0^n = \psi_1^n, \quad \psi_M^n = 0. \tag{9}$$

They are just a translation to discrete level of the boundary conditions (5).

For the most relevant case of cubic nonlinearity, $f(|\psi|^2) = |\psi|^2$, the discrete preserved energy may be obtained in a similar way as N^n and it may be written in the form

$$E^n = -\sum_{j=1}^{M-1} h\left(hj + \frac{h}{2}\right)\frac{1}{2}\left(\left|\frac{\psi_{j+1}^{n+1} - \psi_j^{n+1}}{h}\right|^2 + \left|\frac{\psi_{j+1}^n - \psi_j^n}{h}\right|^2\right) + \sum_{j=1}^{M} h(hj)|\psi_j^{n+1}|^2\frac{|\psi_j^n|^2}{2}. \tag{10}$$

The existence of the conservation law for N^n ensures a good behaviour of the scheme. Following the ideas of Zhang et al. [15], let us study the convergence of the scheme. First we represent by $\Psi^n(r)$ the exact solution at time $t = n\tau$, $\psi^n(r)$ the numerical solution and $\eta^n(r)$ the error at time $n\tau$. We have,

$$\psi^n(r) = \Psi^n(r) + \eta^n(r). \tag{11}$$

Let us define the following innerproduct and associated norm for any functions $u(r)$ and $v(r)$:

$$\langle u, v\rangle = \sum_{j=1}^{M} h^2 j\bar{u}_j v_j, \tag{12}$$

$$\|u\|^2 = \sum_{j=1}^{M} h^2 j|u_j|^2. \tag{13}$$

From the conservation law (8) we have

$$\|\psi^n\|^2 \leqslant N^n = N^0 = \|\Psi^0\|^2 + \|\Psi^1\|^2. \tag{14}$$

The error can be estimated through

$$\|\eta^n\|^2 = \|\psi^n - \Psi^n\|^2 \leqslant 2\|\psi^n\|^2 + 2\|\Psi^n\|^2 \leqslant 2(\|\Psi^0\|^2 + \|\Psi^1\|^2) + \frac{N}{\pi} + 2N^0 + \frac{N}{\pi}, \tag{15}$$

since

$$\|\Psi^n\|^2 \leqslant \int \mathrm{d}r\, r|\Psi(r,n\tau)|^2 = \frac{N}{2\pi}. \tag{16}$$

On the other hand we have that Ψ^n satisfies Eq. (7) with a local truncation error F_j^n of order $O(\tau^2+h^2)$, combining that with (7) we obtain the following equation for the errors:

$$\begin{aligned} &\mathrm{i}\left(\frac{\eta_j^{n+1}-\eta_j^{n-1}}{2\tau}\right)+\frac{\eta_{j+1}^{n+1}-2\eta_j^{n+1}+\eta_{j-1}^{n+1}}{2h^2}+\frac{\eta_{j+1}^{n-1}-2\eta_j^{n-1}+\eta_{j-1}^{n-1}}{2h^2}\\ &\quad+\frac{1}{hj}\left(\frac{\eta_{j+1}^{n+1}-\eta_{j-1}^{n+1}}{4h}\right)+\frac{1}{hj}\left(\frac{\eta_{j+1}^{n-1}-\eta_{j-1}^{n-1}}{4h}\right)+\frac{1}{2}G(|\eta_j^n|^2)(\eta_j^{n+1}+\eta_j^{n-1})\\ &\quad=G_j^n+F_j^n, \end{aligned} \tag{17}$$

where

$$\begin{aligned} G_j^n=&\frac{1}{2}[G(|\Psi_j^n|^2)-G(|\psi_j^n|^2)](\Psi_j^{n+1}+\Psi_j^{n-1})+\frac{1}{2}[G(|\eta_j^n|^2)-G(|\psi_j^n|^2)]\\ &\times(\eta_j^{n+1}+\eta_j^{n-1}). \end{aligned} \tag{18}$$

We now multiply expression (17) by $(\bar{\eta}_j^{n+1}+\bar{\eta}_j^{n-1})/2$, take the imaginary part and sum for all values of j in the spatial mesh to obtain

$$\frac{\|\eta^{n+1}\|^2-\|\eta^{n-1}\|^2}{2\tau}=\mathrm{Im}\Big(\langle\eta_j^{n+1}+\eta_j^{n-1},G^n+F^n\rangle\Big). \tag{19}$$

From here we get

$$\begin{aligned} \|\eta^{n+1}\|^2=&\|\eta^{n-1}\|^2+2\tau\Big[\mathrm{Im}\Big(\langle\eta_j^{n+1}+\eta_j^{n-1},G^n\rangle\Big)\\ &+\mathrm{Im}\Big(\langle\eta_j^{n+1}+\eta_j^{n-1},F^n\rangle\Big)\Big], \end{aligned} \tag{20}$$

and finally,

$$\|\eta^{n+1}\|^2\leqslant(1+2\tau)\|\eta^{n-1}\|^2+2\tau\|\eta_j^{n+1}\|^2+\tau\|F^n\|^2+\tau\|G^n\|^2. \tag{21}$$

Let us now focus on the analysis of the last term of Eq. (21). Let us decompose

$$G_j^n=A_j^n+B_j^n, \tag{22}$$

where

$$A_j^n=\frac{1}{2}[G(|\Psi_j^n|^2)-G(|\psi_j^n|^2)](\Psi_j^{n+1}+\Psi_j^{n-1}) \tag{23}$$

and,

$$B_j^n=\frac{1}{2}[G(|\eta_j^n|^2)-G(|\psi_j^n|^2)](\eta_j^{n+1}+\eta_j^{n-1}). \tag{24}$$

Let us suppose, for instance, that the function G is Lipschitz with constant L (this is a fairly general situation and furthermore this holds in the special cubic case we deal with below). We have

$$\begin{aligned}|A_j^n| &\leqslant \frac{1}{2}L\left||\Psi_j^n|^2 - |\psi_j^n|^2\right|\left|\Psi_j^{n+1} + \Psi_j^{n-1}\right| \\ &\leqslant \frac{1}{2}L|\eta_j^n|\left(|\Psi_j^n| + |\psi_j^n|\right)\left|\Psi_j^{n+1} + \Psi_j^{n-1}\right|. \end{aligned} \tag{25}$$

From here we have

$$\begin{aligned}\|A^n\|^2 &\leqslant \frac{1}{4}\frac{L^2}{h^4}\|\eta^n\|^2\||\Psi_j^n| + |\psi_j^n|\|^2\|\Psi_j^{n+1} + \Psi_j^{n-1}\|^2 \\ &\leqslant \frac{1}{4}\frac{L^2}{h^4}\|\eta^n\|^2\left(\|\Psi_j^n\| + \|\psi_j^n\|\right)^2\left(\|\Psi_j^{n+1}\|^2 + \|\Psi_j^{n-1}\|^2\right) \\ &\leqslant \frac{1}{4}\frac{L^2}{h^4}\|\eta^n\|^2\left(\sqrt{\frac{N}{2\pi}} + \sqrt{N^0}\right)^2\frac{2N}{2\pi}. \end{aligned} \tag{26}$$

On the other hand

$$\begin{aligned}|B_j^n| &\leqslant \frac{1}{2}L\left||\eta_j^n|^2 - |\psi_j^n|^2\right|\left|\eta_j^{n+1} + \eta_j^{n-1}\right| \\ &\leqslant \frac{1}{2}L|\Psi^n|\left(|\eta_j^n| + |\psi_j^n|\right)\left|\eta_j^{n+1} + \eta_j^{n-1}\right|, \end{aligned} \tag{27}$$

and we have

$$\begin{aligned}\|B^n\| &\leqslant \frac{1}{4}\frac{L^2}{h^4}\|\Psi^n\|^2\||\eta^n| + |\psi^n|\|^2\|\eta^{n+1} + \eta^{n-1}\|^2 \\ &\leqslant \frac{1}{4}\frac{L^2}{h^4}\|\Psi^n\|^2(\|\eta^n\| + \|\psi^n\|)^2(\|\eta^{n+1}\|^2 + \|\eta^{n-1}\|^2) \\ &\leqslant \frac{1}{2}\frac{L^2}{h^4}\frac{N}{2\pi}(\|\eta^n\|^2 + N^0)(\|\eta^{n+1}\|^2 + \|\eta^{n-1}\|^2). \end{aligned} \tag{28}$$

So finally

$$\begin{aligned}\|G^n\|^2 &\leqslant \frac{1}{4}\frac{L^2}{h^4}\|\eta^n\|^2\left(\sqrt{\frac{N}{2\pi}} + \sqrt{N^0}\right)^2\frac{2N}{2\pi} + \frac{1}{2}\frac{L^2}{h^4}\frac{N}{2\pi}(\|\eta^n\|^2 + N^0) \\ &\quad \times (\|\eta^{n+1}\|^2 + \|\eta^{n-1}\|^2) \\ &= \frac{C_1}{h^4}\|\eta^n\|^2 + \frac{C_2}{h^4}(\|\eta^{n+1}\|^2 + \|\eta^{n-1}\|^2) + \frac{C_3}{h^4}\|\eta^n\|^2(\|\eta^{n+1}\|^2 + \|\eta^{n-1}\|^2). \end{aligned} \tag{29}$$

Substituting in (21) we have

$$\|\eta^{n+1}\|^2 \leqslant (1+2\tau)\|\eta^{n-1}\|^2 + 2\tau\|\eta_j^{n+1}\|^2 + \tau\|F^n\|^2 + \frac{\tau C_1}{h^4}\|\eta^n\|^2 + \frac{\tau C_2}{h^4} \times (\|\eta^{n+1}\|^2 + \|\eta^{n-1}\|^2) + \frac{\tau C_3}{h^4}\|\eta^n\|^2(\|\eta^{n+1}\|^2 + \|\eta^{n-1}\|^2). \tag{30}$$

We now sum up this expression from $n = 1$ to some final value $n = J - 1$, and rearranging terms we get

$$\begin{aligned}(1-\tau\kappa_1)\|\eta^J\|^2 + (1+\tau\kappa_1)\|\eta^{J-1}\|^2 + \tau\kappa_2\|\eta^J\|^2\|\eta^{J-1}\|^2 \\ \leqslant (1-\tau\kappa_1)\|\eta^1\|^2 + (1+\tau\kappa_1)\|\eta^0\|^2 + \tau\kappa_2\|\eta^1\|^2\|\eta^0\|^2 \\ + 2\tau\kappa_2\sum_{n=2}^{J}\|\eta^n\|^2\|\eta^{n-1}\|^2 + \tau\kappa_3\sum_{n=1}^{J-1}\|\eta^n\|^2 + \tau\sum_{n=1}^{J-1}\|F^n\|^2,\end{aligned} \tag{31}$$

with

$$\kappa_1 = \left(2 + \frac{C_2}{h^4}\right), \quad \kappa_2 = \frac{C_3}{h^4}, \quad \kappa_3 = \left(4 + \frac{C_1 + 2C_2}{h^4}\right). \tag{32}$$

Using (15) we have

$$\|\eta^J\|^2 \leqslant \|\eta^1\|^2 + \frac{1+\tau\kappa_1}{1-\tau\kappa_1}\|\eta^0\|^2 + \tau\frac{\kappa_2}{1-\tau\kappa_1}\|\eta^1\|^2\|\eta^0\|^2 + \tau\frac{1}{1-\tau\kappa_1} \times \sum_{n=1}^{J-1}\|F^n\|^2 + \tau\frac{\kappa_3+\kappa_4}{1-\tau\kappa_1}\sum_{n=1}^{J-1}\|\eta^n\|^2, \tag{33}$$

with

$$\kappa_4 = 2\kappa_2\left(2N^0 + \frac{N}{\pi}\right). \tag{34}$$

Finally let us consider the following Lemma [26]:

Lemma 1. *Let $\omega(k)$ and $\rho(k)$ be nonnegative mesh functions. If $C > 0$ and $\rho(k)$ is nondecreasing, and the inequality,*

$$\omega(k) \leqslant \rho(k) + \tau C\sum_{j=0}^{k-1}\omega(j),$$

holds for all k, then for all k

$$\omega(k) \leqslant \rho(k)\mathrm{e}^{Ckt}.$$

We apply the Lemma with

$$k = J, \quad \omega(J) = \|\eta^J\|^2, \quad C = \frac{\kappa_3 + \kappa_4}{1 - \tau\kappa_1},$$

$$\rho(J) = \|\eta^1\|^2 + \frac{1 + \tau\kappa_1}{1 - \tau\kappa_1}\|\eta^0\|^2 + \tau\frac{\kappa_2}{1 - \tau\kappa_1}\|\eta^1\|^2\|\eta^0\|^2 + \tau\frac{1}{1 - \tau\kappa_1} \times \sum_{n=1}^{J-1}\|F^n\|^2. \tag{35}$$

We conclude that if τ is small enough so that $C > 0$, we have

$$\|\eta^J\|^2 \leqslant \left(\|\eta^1\|^2 + \frac{1 + \tau\kappa_1}{1 - \tau\kappa_1}\|\eta^0\|^2 + \tau\frac{\kappa_2}{1 - \tau\kappa_1}\|\eta^1\|^2\|\eta^0\|^2\right)\mathrm{e}^{CJt}. \tag{36}$$

This means that the numerical error is bounded by the initial and truncation errors, so the scheme is convergent. The stability with respect to initial and roundoff errors can be established in a similar way.

3. The self-adaptive algorithm

Up to this point we have developed a conservative, second-order numerical scheme which is linearly implicit and has good convergence properties. This point is very important and it was one of our goals since nonlinearly implicit schemes need an inner iteration which requires several times more computation and generates the problem of the proper choice of the method of solution of the system of nonlinear equations. On the contrary, our implicit method requires the solution of only one linear system per step. This fact, together with the good properties of the system matrix, may be used to solve the problem using a multigrid algorithm.

Additionally, to follow collapse (or quasi-collapse) events with high precision, one must be able to keep information at the same time on the very small scale where the spike is localized and on the large scale which hosts the non-collapsing part of the solution. Very fine grids, which are needed in order to obtain accurate and reliable numerical solutions require a very large number of operations and memory requirements. However, the discretization error is usually different in different parts of the simulation domain, as in problems with singularities, boundary layers, etc., so the use of globally uniform grids involves a waste of computational resources. Therefore, high accuracy may be obtained by using finer grids in the regions of the computational domain where it is necessary and maintaining coarser grids covering the whole domain. This approach considerably reduces the computer time requirements of a simulation code. Also the time step must be controlled when the amplitude of the solution is growing very fast in a particular region of the computational domain. We

have implemented all of these features in a code which we now describe and whose general view is shown in Fig. 1.

The fully self-adaptive method used to study the behavior of the solution in the neighborhood of the singularity, combines automatic generation of girds, multigrid techniques and a self-adaptive time step. A refinement criterion places finer grids where the solution is difficult to approximate, maintaining coarser grids on the rest of the simulation region. So, the solution is reached with much lower computational work and memory requirements for a given accuracy. As a matter of fact, it allows us to perform simulations with accuracy not obtainable on current computers using global grids. This technique has been previously applied by some of us to solve efficiently other physical problems also related to the NLSE [28].

A hierarchy of global grids is typically designed as $\Omega_1, \Omega_2, \ldots, \Omega_m$, where 2^m is the number of points in the grid. Our approach uses a hierarchy of grids designed as $\Omega', \Omega'_2, \ldots, \Omega'_m$, where $\Omega_m \subseteq \Omega'_m$ (i.e. Ω'_m covers part of Ω_m). This hierarchy of partial grids is constructed in a fully automatic way under a refinement criterion. The process starts from two coarser grids that cover the whole domain. The refinement criterion decides the part of the domain that the next finer grid must cover. This decision is made by estimating the truncation error with the solution on current and next coarser grids. Following this rule, the error is compared with a tolerance given as an input parameter to the code. This refinement process is successively performed until the criterion is globally

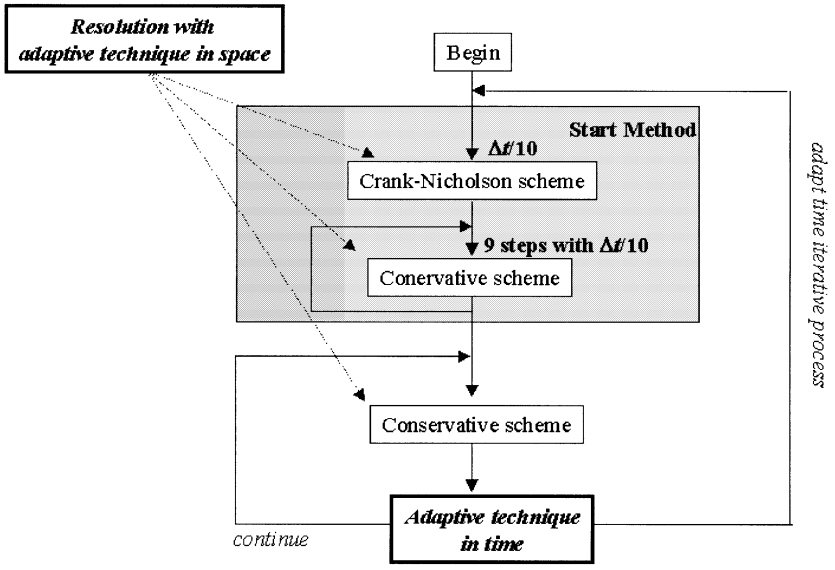

Fig. 1. Schematic view of the code implementing the numerical scheme.

satisfied. This grid is always extended to build a power of two grid in order to implement a multigrid algorithm (Fig. 2).

The discrete operator is solved on each partial grid considering the extreme points as boundary conditions, with an initial guess given by the interpolation of the solution in the next coarser grid. The tridiagonal system of equations is solved by a multigrid-type iterative method. So, the global algorithm is similar to a full multigrid method but refining just where higher accuracy is required. The multigrid algorithm is used as an internal solver due to its optimal complexity and architectural properties (parallelism and data locality) [29]. The code has been parallelized with the standard OpenMP directives for shared-memory parallel computing on a 32-processor SGI Origin 2000. Other solvers like the Thomas algorithm (tridiagonal Gaussian elimination) could be applied on a sequential computer. The algorithm is not as efficient as the MLAT method [30] because the boundary conditions for a partial grid remain fixed in the correction process.

The time-dependence of the partial differential equations adds a difficulty in the self-adaptive resolution process. The numerical method needs the solution in the two previous time steps to compute the new time step. We have to consider that the adaptive grids are dynamically constructed in execution time and so a different adaptive grid hierarchy is used in each step. The numerical scheme may need the solution in a given grid level of a part of the domain that was not computed in previous time steps. This is why our scheme also incorporates interpolation operators to estimate the solution on the points which are required and where not computed previously.

As simulation time tends to the blow-up time, the solution collapses and approaches the singularity. A fixed time step (τ) is not capable of following the solution in the neighborhood of the singularity because the simulation exceeds the blow-up time. Our algorithm uses a self-adaptive time step algorithm to guide the simulation near the singularity. The decision of when the time step is refined is made by comparing the growth rate of the amplitude of the discrete solution in the two previous time steps. If the rate decreases (this is the coarsest way to know that something goes wrong), the time step is adapted and the last time steps are undone (Fig. 1). Another way to control the step could be the use of the virial identities to be presented later.

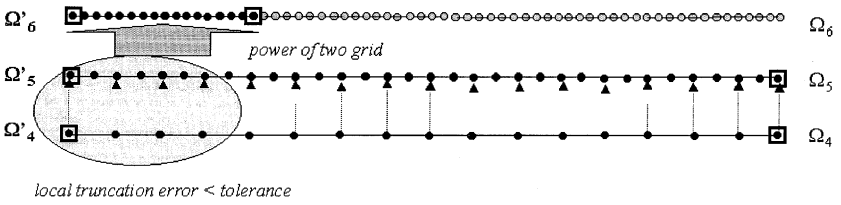

Fig. 2. The multigrid algorithm.

4. Applications to the cubic nonlinearity case

4.1. The test problem

To evaluate the behaviour of the numerical scheme we have chosen a problem for which many things are known despite its nonintegrable character, which is that of the collapse in the two-dimensional cubic NLSE. In this way we may evaluate the applicability of the method for the solution of other, less known problems. Thus we will concentrate in the cubic nonlinearity case, $f(|\Psi|^2) = |\Psi|^2$ and $n = 2$.

4.2. Generalities

Particular global solutions of Eq. (2) are nonlinear bound states of the form

$$\Psi_\omega(\mathbf{x}, t) = \varphi_\omega(\mathbf{x})\mathrm{e}^{\mathrm{i}\omega t}. \tag{37}$$

In order to guarantee the existence of nonlinear bound states the potential $U(\Psi)$ has to be attractive, i.e., $U(\Psi) < 0$ for some $\Psi \in X$. Of particular interest are the so-called ground states which are nonlinear bound states which can be obtained by solving an appropriate minimization problem and have least energy among all nontrivial quasi-stationary solutions of the form (37).

If we consider the particular case of the power nonlinearity $f(\Psi) = |\Psi|^{2p}$, since the energy $E(\Psi)$, and norm $N(\Psi)$ are conserved, all the solutions $\Psi \in X$ satisfy

$$\begin{aligned} &K(\Psi) = E(\Psi_0) - U(\Psi) \leq E(\Psi_0) + cN(\Psi_0)^{\beta p} K(\Psi)^{(1-\beta)p+1}, \\ &\quad c > 0, \;\; \beta = \frac{1}{p} - \frac{n-2}{2}, \end{aligned} \tag{38}$$

by Hölder's and Sobolev's inequalities [31]. We obtain then the following inequality:

$$\frac{K(t) - E}{K^{(np)/2}} \leqslant cN^{(p+1-(np)/2)}. \tag{39}$$

It is clear that if $pn < 2$, for inequality (39) to be valid it is necessary that $K(t)$ is bounded in X for all times and thus all the solutions are global. For the critical case $pn = 2$, separate analysis is necessary and it is found [31] that if $N(\Psi_0) < N(\varphi_1)$, φ_1 being the ground state with frequency 1, then the solution of the Cauchy problem is global. On the other hand, for $pn = 2$, there exists solutions which blow-up in finite time in the sense that

$$\lim_{t \uparrow T} K(\Psi(t)) \to \infty \quad \text{for } T < \infty, \tag{40}$$

or, in other words, their H^1 norm diverges. It is also known that for each $\omega > 0$, Eq. (2) has an unique ground state solution, which is stable in the case $pn < 2$, and unstable if $pn > 2$.

More information on global existence can be obtained from the variance identity (also called virial theorem). Let us define

$$W(t)^2 = \frac{4}{N} \int \mathrm{d}^n \mathbf{x} r |\Psi|^2, \tag{41}$$

where $r = \|\mathbf{x}\|^2$. W^2 is the second moment of the distribution Ψ, and has the physical meaning related to the width of the wavepacket (provided it has zero mean). Its evolution may be found to be [32]

$$W(t)^2 = W_0^2 + 2\frac{W_0^2}{R_0} t + (\Theta_0^2 - 8J_0)t^2, \tag{42}$$

where

$$\Theta^2 = -\frac{16\pi}{N} \int_0^\infty r\Psi(r) \left[\frac{\partial^2 \bar{\Psi}}{\partial r^2} + \frac{1}{r} \frac{\partial \bar{\Psi}}{\partial r} \right] \mathrm{d}r, \tag{43a}$$

$$\frac{1}{R} = \mathrm{i}\frac{4\pi}{NW^2} \int_0^\infty \left[\frac{\partial \Psi}{\partial r} \bar{\Psi}(r) - \Psi(r) \frac{\partial \bar{\Psi}(r)}{\partial r} \right] r^2 \mathrm{d}r, \tag{43b}$$

$$J = \frac{2\pi}{N} \int_0^\infty |\Psi(r)|^4 r \mathrm{d}r. \tag{43c}$$

and the index 0 indicates the value of those quantities at $t = t_0$. Since $8E = \theta^2 - 8J$, we obtain $\mathrm{d}^2/\mathrm{d}t^2(W) = 8E$. It is easy to see then that all initial data Ψ_0, with negative initial energy such that $x_j \Psi_0 \in L^2(R^n)$, blow-up on or before the finite time t_* for which $W(t_*) = 0$. The known evolution of the wavepacket width (42) provides also another test of the quality of the numerical simulation scheme.

4.3. The rate of the critical blow-up

Let us look for self-similar solutions of the form

$$\Psi(\mathbf{x}, t) = \frac{1}{f(t)} \Phi\left(\frac{\mathbf{x}}{f(t)} \right), \tag{44}$$

with $f(t) \to 0$ as $t \to t_*$. It has been realized in numerical experiments [33] and partially justified later [34] that the only initial data which collapse self-similarly are those satisfying $N(\Psi_0) = N(\varphi_1)$.

In [34] it is also proved that initial data related to the ground state through the expression

$$\Psi_0 = a^{-1}\varphi_1\left(\frac{r}{a}\right)e^{(ibr^2)/4a}e^{(ic)/a}, \tag{45}$$

blow-up in finite time at the origin provided that $ab < 0$. In particular, the time evolution of these data is given by

$$\Psi(r,t) = \frac{1}{a+bt}\varphi_1\left(\frac{r}{a+bt}\right)e^{(ibr^2)/4(a+bt)}e^{(i(c+dt))/(a+bt)}, \tag{46}$$

where $ad - bc = 1$.

The cases in which the equality $N(\Psi_0) = N(\varphi_1)$, is not satisfied the collapse is not fully self-similar but the solution can be separated into a self-similar spike, a transition region and a quasi-stationary region which does not change appreciably near the collapse point but it contributes to a finite width of the solution at the collapse (so collapse occurs before the width becomes zero). The analysis of the problem is then complicated since the solution at different regions must be matched and the exact self-similar solutions which can be found are unstable. A related question concerns the exact form of the rate of blow-up of the self-similar spike, which is different from (50) because of the different spatial structure of the solution, i.e., the analytical form of $f(t)$. The first analysis of this problem was done by Kelley [35], who proposed on the basis of numerical simulations for a Gaussian initial data, a blow-up rate of the type

$$|\Psi(0,t)| \to (t_* - t)^{-1/2}, \quad t \to t_*. \tag{47}$$

Later many other proposals for the asymptotic behavior of this quantity were proposed (for a survey see [4]). The later high precision simulations [36] show that probably the best approach to the singularity can be achieved by using a double logarithmic law of the type

$$|\Psi(0,t)| \to \left[\frac{\log|\log(t_* - t)|}{(t_* - t)}\right]^{1/2}, \quad t \to t_*. \tag{48}$$

Other papers which have contributed to the numerical study of this problem are [37,38].

As it has been already commented before, the most accurate numerical schemes used in the simulation of the collapse process obey to two different philosophies. There is one family of schemes which try to adapt the grid to the solution as it collapses, so that regions where the gradients are higher are represented with higher density grids. This fact allows to keep the number of points in the problem accessible while representing properly the sharp change in the solution. The second way of addressing the problem consists of changing the equation at a chosen self-similar rate and study its variations. However, all of them have serious limitations concerning the precision of the final solution.

We have used this problem as a test for the validity of the scheme proposed in our paper. Specifically in the following subsection we will consider its ap-

plication to the analysis of the critical blow-up and compare with all stabilized results.

4.4. Computation and simulations of the ground state and near states

We have first checked our simulation method taking as initial data the state

$$\Psi(r,0) = \varphi_1(r)\mathrm{e}^{-\mathrm{i}r^2}/4. \tag{49}$$

These data correspond to the one defined in (45) for the particular choice $a = 1$, $b = -1$. This case is interesting because as we mentioned its blow-up rate is known [34] and it is given by

$$f(t) = \frac{\varphi_1(0)}{1-t}. \tag{50}$$

Since the blow-up is completely self-similar it collapses with zero width at the critical time $t_* = 1$.

We have first computed the ground state and its norm. In our particular case $n = 2$, $p = 1$ and radial symmetry, the ground state satisfies the equation

$$\frac{\mathrm{d}^2}{\mathrm{d}r^2}\varphi_1 + \frac{1}{r}\frac{\mathrm{d}}{\mathrm{d}r}\varphi_1 - \varphi_1 + 2\varphi_1^3 = 0. \tag{51}$$

The boundary conditions are

$$\left.\frac{\mathrm{d}\varphi_1}{\mathrm{d}r}\right|_{r=0} = 0, \quad \lim_{r\to\infty}\varphi_1(r) = 0. \tag{52}$$

Eqs. (51), (52) define a boundary value problem. In order to find its solution $\varphi_1(r)$, we use a shooting method. The idea is to rewrite Eq. (51) as the following dissipative dynamical system

$$\frac{\mathrm{d}}{\mathrm{d}r}\varphi_1 = v, \tag{53a}$$

$$\frac{\mathrm{d}}{\mathrm{d}r}v = \varphi_1 - \frac{v}{r} - 2\varphi_1^3. \tag{53b}$$

The solution we search must satisfy the boundary conditions. This means that the initial value for v is $v = 0$ and the value for φ_1 is looked for in order to satisfy that $\lim_{r\to\infty}\varphi_1(r) = 0$.

As is shown in Fig. 3 from the dynamical point of view the ground state is a branch of the stable manifold of the fixed point (0,0). We can only approximate this manifold, since for any initial value $\varphi_1(0)$ considered we do not approach the fixed point (0,0) infinitely. There always exists a time t_0 for which we get away from it and we reach one of the two fixed stable points $(-\sqrt{1/2},0)$ or $(\sqrt{1/2},0)$.

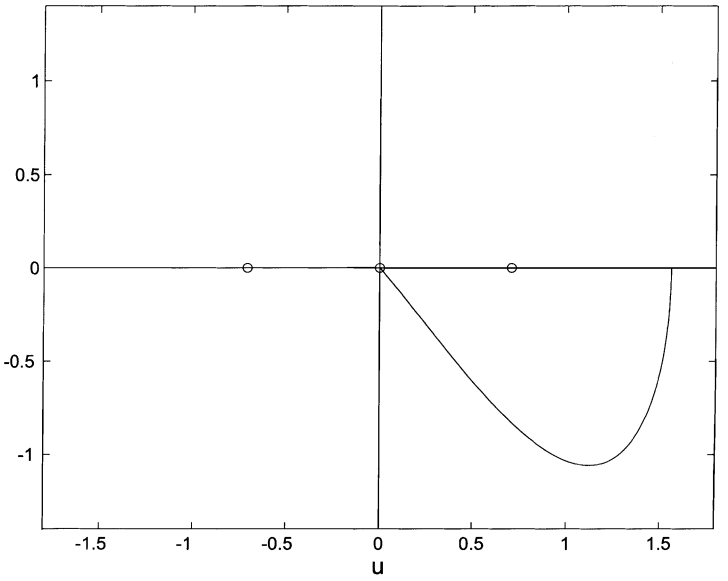

Fig. 3. Projection of the ground state in the phase space. As it is shown the ground state is a branch of the stable manifold of (0,0).

We have calculated the ground state with the Dormand–Prince pair of order 5 incorporated in Matlab. In order to avoid the singularity which appears in (53b) at the starting point $r = 0$ we have solved the indetermination by means of a series expansion of φ_1 around $r = 0$ as follows:

$$\varphi_1(r) = \varphi_1(0) + \varphi_1'(0)r + \frac{1}{2}\varphi_1''(0)r^2 + \mathcal{O}(r^3), \tag{54}$$

which is consistent with the order of the numerical scheme. When expression (54) and boundary conditions are replaced in Eq. (53b) we arrive at first-order at

$$\varphi_1''(0) = \varphi_1(0) - \varphi_1''(0) - 2\varphi_1(0)^3 + \mathcal{O}(r^1). \tag{55}$$

So at the origin we find that $\varphi_1''(0) = (\varphi_1(0) - \varphi_1(0)^3)/2$. Using this boundary approximation we proceed with the approximation scheme to get φ_1 for which we find $\varphi_1(0) = 1.56092093206074$, $\|\varphi_1(r)\| = 2.4186430$, $\Theta_0^2 - 8J_0 = -8.2848 \times 10^{-5}$.

Once we have a numerical approximation of φ_1 we can evaluate for instance the width evolution (42) for the initial data (49). It can be shown that here,

$$\begin{aligned} &W_0^2 = 2.37270256496696, \\ &2\frac{W_0^2}{R_0} = -4.74540512993392, \\ &(\Theta_0^2 - 8J_0) = 2.37261978316741. \end{aligned} \tag{56}$$

As expected in a complete self-similar blow-up, the collapse time predicted for this width is $t_* = 0.9941280$ which is close to the expected $t_* = 1$.

We have integrated the NLSE (4) for the initial data (49), in order to see how our numerical scheme follows the solution blow-up. The starting grid taken is made of 262,144 points, and the initial time step τ is 0.001. With this choice we achieve values of t_* very close to the expected $t_* = 1$. We have made other simulations with initial data very close to (49) which are not collapsing and our simulation does not do so either. At each time step the width is estimated from Eq. (41) and it is compared with the one obtained from (42) with parameters (56). The maximum value of difference between them along the simulation is 10^{-3}.

In order to check that the simulation follows (50), we analyse the values $|\Psi(0,t_i)|$ obtained at each time step t_i. From these numerical data we adjust the law

$$|\Psi(0,t)| = A(t_* - t)^{\alpha}, \tag{57}$$

where the parameters A, α and t_* are expected to be close, respectively, to $\varphi_1(0), -1$ and 1. To perform the fitting we take logarithms in Eq. (57) and we minimize the quadratic difference with respect to all parameters:

$$S_1^2(A,\alpha,t_*) = \sum_i (\ln|\Psi(0,t_i)| - \ln A - \alpha \ln(t_* - t_i))^2, \tag{58}$$

where index i runs all over the data set. The extreme condition of Eq. (58) gives the following equations:

$$\sum_i (-\ln(|\Psi(0,t_i)|) + \ln A + \alpha \ln(t_* - t_i)) = 0, \tag{59}$$

$$\sum_i (-\ln(|\Psi(0,t_i)| + \ln A + \alpha \ln(t_* - t_i)) \ln(t_* - t_i)) = 0, \tag{60}$$

$$\sum_i \left(\frac{-\ln(|\Psi(0,t_i)|) + \ln A + \alpha \ln(t_* - t_i)}{t_i - t_*} \right) = 0. \tag{61}$$

This is a linear set of equations on the parameters $\ln A$ and α and nonlinear in t_*. If parameters $\ln A$ and α are expressed as functions of t_* then the system is transformed in a nonlinear equation which can be solved for t_* with a Newton method. These quantities minimize S_1^2 but not necessarily S^2 which is defined as follows:

$$S^2 = \frac{\sum_i (|\Psi(0,t_i)|_{\mathrm{n}} - |\Psi(0,t_i)|_{\mathrm{a}})^2}{N_{\mathrm{s}}}. \tag{62}$$

Here $|\Psi(0,t_i)|_{\mathrm{n}}$ are the numerical values obtained from the simulation while $|\Psi(0,t_i)|_{\mathrm{a}}$ are the adjusted values and N_{s} is the number of steps in the simulation. Once the parameters that minimize Eq. (58) have been adjusted we use

them as a starting point in order to minimize S^2. We use for that the Matlab `nlinfit` and `nlparci` commands which provides, respectively, the nonlinear fit and the confidence intervals at 95% of the adjusted parameters. The results for the parameters of the fit for the Gaussian initial data are $t_* = 1.0232 \pm 0.0007 \times 10^{-4}$, $A = 1.477 \pm 0.011$, $\alpha = -1.125 \pm 0.007$, $S = 0.21$, $s = 0.0052$, where S which is the square root of S^2 and s defined as $s = S/|\Psi(0, t_{\max})|$. We see that the results agree with the theoretical expectatives.

4.5. Verification of the double logarithmic law

We have also considered the evolution of the Gaussian initial data

$$\Psi(r, 0) = P\mathrm{e}^{-r^2/W_0^2}, \tag{63}$$

where $P = 0.124264$ and $W_0^2 = 100.00$ The double logarithmic law (48) is the most appropriate to describe its evolution as [36] shows.

The width evolution (42) of a Gaussian is given by

$$W^2 = W_0^2 + \left(\frac{16}{W_0^2} - 4P^2\right)t^2. \tag{64}$$

For the values (P, W_0^2) chosen it is easy to show that there is a finite collapse time. However at this time the initial data do not have a zero width because the blow-up is not fully self-similar.

We have integrated the NLSE for the Gaussian data considering a starting grid size of 524,288 points and an initial time step $\tau = 0.001$. In this case the maximum value obtained for t is

$$t_{\max} = 6.711417038 \pm 4 \times 10^{-9},$$

where the amplification of $|\Psi(0, 0)|^2$ is of order 10^{10}. For other choices in the size of the grid and time step, amplifications of order 10^{13} can be reached.

We have adjusted the values $|\Psi(0, t_i)|$ obtained at each time step to the double logarithmic law (48). As before, we first minimize the quadratic differences of the logarithm of the law and then we use these results as a starting point for the Matlab `nlinfit` and `nlparci` routines. Using this we find $A = 1.362 \pm 0.021$, $S = 77.02$ and $s = 0.0059$. It must be noticed that the adjustment is not performed for all data but only for those values $t > 6.7$ in which the self-similar regime for the spike is presumably reached. In order to confirm the validity of the model we use the cross validation method. It consists of representing the values of the amplitudes obtained in the simulation versus the predicted ones in those points. This should be a straight line of slope $m = 1$ and ordinate at the origin, $a = 0$. The estimations of these parameters using the numerical data are $m = 0.9949 \pm 0.0068$ and 16.20 ± 25.18. We also provide

the semi amplitude of the 95% confidence interval. They are consistent with the null hypothesis ($m = 1$, $a = 0$).

5. Conclusions

In this paper we have developed a new adaptive multigrid finite difference scheme useful for the analysis of wave collapse processes. This scheme is linearly implicit, which allows a fast implementation, and conservative, which is a desirable property of any numerical scheme which is to be used in the simulation of Hamiltonian wave equations.

As a test of validity of the ideas beyond our scheme, we have applied it to the simulation of collapse processes in the critical NLSE. In this context we have verified the width evolution, which satisfies the virial identities and the rate of self-similar collapse near the singularity. The scheme is able to follow numerically the collapse process up to amplifications of 10^{13} and to determine the collapse time with high precision.

These schemes may be used to approximate many other collapse phenomena related to recent problems, e.g., nonlocal collapses in Bose–Einstein condensation [39], collapses in saturable media, etc. We expect that this will be a useful tool in future investigations of blow-up phenomena in context of NLSEs.

Acknowledgements

We want to acknowledge Miguel A. Porras, Jorge Mateu, Pilar Grau and Guo Ben Yu for discussions. IM is partially supported by CICYT grant TIC 99/0474. VMPG is partially supported by the Ministerio de Ciencia y Tecnología under grant BFM2000-0521. LV is partially supported by the Ministerio de Ciencia y Technología under grant PB98-0850. The authors wish to thank CSC (Centro de Supercomputación Complutense) for providing access to its parallel computer facilities.

References

[1] A. Hasegawa, Optical Solitons in Fibers, Springer, Berlin, 1989.
[2] R.K. Dodd, J.C. Eilbeck, J.D. Gibbon, H.C. Morrin, Solitons and Nonlinear Wave Equations, Academic Press, New York, 1982.
[3] A.S. Davydov, Solitons in Molecular Systems, Reidel, Dordrecht, 1985.
[4] C. Sulem, P. Sulem, The Nonlinear Schrödinger Equation, Springer, Berlin, 2000.
[5] F. Dalfovo, S. Giorgini, L.P. Pitaevskii, S. Stringari, Theory of Bose–Einstein Condensation in Trapped Gases, Rev. Mod. Phys. 71 (1999) 463–512.
[6] C.C. Bradley, C.A. Sackett, J.J. Tollett, R.G. Hulet, Evidence of Bose–Einstein condensation in an atomic gas with attractive interactions, Phys. Rev. Lett. 75 (1995) 1687–1691.

[7] T. Tsurumi, H. Morise, M. Wadati, Stability of Bose–Einstein condensates confined in traps, Int. J. Mod. Phys. 14 (2000) 655–719.
[8] J. Ginibre, G. Velo, On a class of nonlinear Schrödinger equations. I. The Cauchy problem, general case, J. Funct. Anal. 32 (1979) 1–32.
[9] M.J. Landman, G.C. Papanicolau, C. Sulem, P.L. Sulem, X.P. Wang, Stability of isotropic singularities for the nonlinear Schrödinger equation, Physica D 47 (1991) 393–415.
[10] T.R. Taha, M.J. Ablowitz, Analytical and numerical aspects of certain nonlinear evolution equations II. Numerical, nonlinear Schrödinger equation, J. Comput. Phys. 55 (1984) 203–230.
[11] B.M. Herbst, J.Ll. Morris, A.R. Mitchell, Numerical experience with the nonlinear Schrödinger equation, J. Comput. Phys. 60 (1985) 282–305.
[12] M. Delfour, M. Fortin, G. Payre, Finite difference solutions of a nonlinear Schrödinger equation, J. Comput. Phys. 44 (1981) 277–288.
[13] J.M. Sanz-Serna, J.G. Verwer, Conservative and nonconservative schemes for the solution of the nonlinear Schrödinger equation, IMA J. Numer. Anal. 6 (1986) 25–42.
[14] L.S. Peranich, A finite difference scheme for solving a nonlinear Schrödinger equation with a linear damping term, J. Comput. Phys. 68 (1987) 501–505.
[15] F. Zhang, V.M. Pérez-García, L. Vázquez, Numerical simulation of nonlinear Schrödinger systems: A new conservative scheme, Appl. Math. Comput. 71 (1995) 164–177.
[16] W.A. Strauss, L. Vazquez, Numerical solution of a nonlinear Klein–Gordon equation, J. Comput. Phys. 28 (1978) 271–278.
[17] Y. Tang, L. Vázquez, F. Zhang, V.M. Pérez-García, Symplectic methods for the nonlinear Schrödinger equation, Comput. Math. Appl. 32 (1996) 73–83.
[18] Y. Tang, V.M. Pérez-García, L. Vázquez, Symplectic methods for the Ablowitz–Ladik model, Appl. Math. Comput. 82 (1997) 17–38.
[19] O. Karakashian, C. Makridakis, A space-time finite element method for the nonlinear Schrödinger equation: The discontinuous Galerkin method, Math. Comput. 67 (1998) 479–499.
[20] Y. Tourigny, J. Morris, An investigation into the effect of product approximation in the numerical solution of the cubic nonlinear Schrödinger equation, J. Comput. Phys. 76 (1988) 103–130.
[21] J.A.C. Weideman, B.M. Herbst, Split-step methods for the solution of the nonlinear Schrödinger equation, SIAM J. Numer. Anal. 23 (1986) 485–507.
[22] D. Pathria, J.Ll. Morris, Pseudo-spectral solution of nonlinear Schrödinger equations, J. Comput. Phys. 87 (1990) 108–125.
[23] A.D. Bandrauk, H. Shen, High-order split-step exponential methods for solving coupled nonlinear Schrödinger equations, J. Phys. A: Math. Gen. 27 (1994) 7147–7155.
[24] B.M. Herbst, F. Varadi, M.J. Ablowitz, Symplectic methods for the nonlinear Schrödinger equation, Math. Comput. Simul. 37 (1994) 353–369.
[25] R. MacLahan, Symplectic integration of Hamiltonian wave equations, Numer. Math. 66 (1994) 465–492.
[26] F. Zhang, L. Vázquez, Two energy-conserving numerical schemes for the Sine–Gordon equation, Appl. Math. Comput. 45 (1991) 17–29.
[27] S. Jiménez, Derivation of the discrete conservation laws for a family of finite difference schemes, Appl. Math. Comput. 64 (1994) 13–45.
[28] I.M. Llorente, F. Tirado, L. Vázquez, J.C. Fabero, A self-adaptive approach to the parallel numerical simulation of the nonlinear Schrödinger equation using multigrid techniques, in: 6TH Joint EPS-APS International Conference on Physics Computing, Lugano, Switzerland, European Physical Society Press, Geneva, 1994, pp. 151–154.
[29] I.M. Llorente, F. Tirado, Relationships between efficiency an execution time of full multigrid methods on parallel computers, IEEE Trans. Parallel Distrib. Syst. 8 (1997) 562–573.

[30] A. Brandt, Multi-level adaptive solutions to boundary-value problems, Math. Comput. 31 (1977) 343–400.
[31] M.I. Weinstein, Nonlinear Schrodinger equations and sharp interpolation estimates, Commun. Math. Phys. 87 (1983) 567–576.
[32] M.A. Porras, J. Alda, E. Bernabeu, Nonlinear propagation and transformation of arbitrary laser beams by means of the generalized ABCD formalism, Appl. Opt. 32 (1993) 5885–5991.
[33] K. Rypdal, J.J. Rasmussen, K. Thomsen, Similarity structure of wave collapse, Physica D 16 (1985) 339–357.
[34] M.I. Weinstein, On the structure and formation of singularities in solutions to nonlinear dispersive evolution equations, Commun. Partial Differential Equation 11 (1986) 545–565.
[35] P.L. Kelley, Self-focusing of optical beams, Phys. Rev. Lett. 15 (1965) 1005–1008.
[36] G.D. Akrivis, V.A. Dougalis, O.A. Karakashian, W.R. McKinney, Numerical approximation of blow-up of radially symmetric solutions of the nonlinear Schrödinger equation, SIAM J. Sci. Comput. (1999), submitted.
[37] N.E. Kosmatov, V.F. Shvets, V.E. Zaharow, Computer simulation of wave collapses in the nonlinear Schrödinger equation, Physica D 52 (1991) 16–35.
[38] Y. Touringuy, J.M. Sanz Serna, The numerical study of blow-up with application to a nonlinear Schrödinger equation, J. Comput. Phys. 102 (1992) 407–416.
[39] V.M. Pérez-García, V. Konotop, J.J. García-Ripoll, Dynamics of quasi-collapse in nonlinear Schrödinger systems with nonlocal interactions, Phys. Rev. E 62 (2000) 4300–4308.